Inorganic Chemistry

Article

pubs.acs.org/IC

Directional Energy Transfer in Mixed-Metallic Copper(I)−Silver(I) Coordination Polymers with Strong Luminescence

Seiko Shibata,[†] Kiyoshi Tsuge,*[,‡] Yoichi Sasaki,*[,†] Shoji Ishizaka,[§] and Noboru Kitamura[†]

[†]Division of Chemistry, Faculty of Science, Hokkaido University, Kita-ku, Sapporo 060-0810, Japan

[‡]Graduate School of Science and Engineering, University of Toyama, Toyama, Toyama 930-8555, Japan

[§]Graduate School of Science, Hiroshima University, Higashi-Hiroshima, Hiroshima 739-8526, Japan

Supporting Information

ABSTRACT: Strongly luminescent mixed-metallic copper(I)−silver(I) coordination polymers with various Cu/Ag ratio were prepared by utilizing the isomorphous relationship of the luminescent parent homometallic coordination polymers (Φ_{em} = 0.65 and 0.72 for the solid Cu and Ag polymers, respectively, at room temperature). The mixed-metallic polymer with the mole fraction of copper even as low as 0.005 exhibits a strong emission (Φ_{em} = 0.75) from only the copper sites as the result of the efficient energy migration from the silver to the copper sites. The migration rates between the two sites were evaluated from the dependence of emission decays upon the mole fraction of copper.

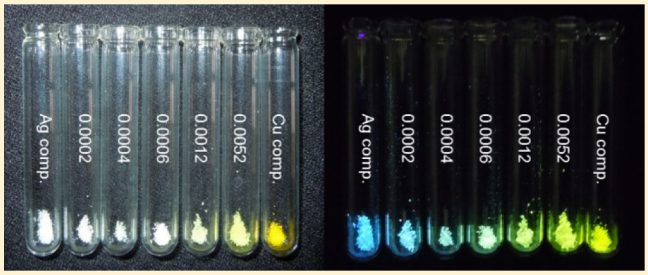

INTRODUCTION

Energy migration among chromophores and energy transfer to acceptors are essential processes in the light-harvesting units in the natural and artificial photosynthesis systems,[1,2] which have been receiving growing interest and are finding applications for solar cells[3,4] and light-emitting diodes.[5] The beautiful arrangement of chlorophyll pigments in natural light-harvesting systems[6] is favorable to efficient energy transfer, and has been stimulating researchers to construct artificial systems with similar functions by integrating chromophores through covalent and noncovalent interactions.[7−16] Direct linkage of chromophores by covalent interaction has produced dendrimers,[10,11] extended systems formed by a combination of π-conjugated units,[12] and polymers with pendant dye groups.[13] Approaches using intermolecular noncovalent interactions yielding supramolecular aggregates are also attractive, as represented by the SAMs and layer materials[17,18] and by organogels constructed by hydrogen bonds and $\pi-\pi$ stacking interactions.[19] The combination of dyes and nanoporous materials such as zeolites[7] and periodic mesoporous silica[8,9] can be also classified for the exploration of the intermolecular noncovalent interaction.

For the construction of the antenna system, not only the choice of chromophores but also their precise arrangement is essential. Coordination bond has been proved to be an excellent tool for that purpose, as observed in metal−organic frameworks or coordination polymers.[20] Recently, the study of coordination polymers was extended to mixed-component crystals or solid solutions by taking advantage of the isomorphous relationship of parent crystals or structural similarity of units.[21−23] The formation of solid solutions or "doping" has been widely utilized in the solid-state metal and metal compounds, such as alloys, semiconductors, and phosphors.[24] A wide variety of available units in the coordination chemistry promotes the modification of structures[25] and the improvement of the properties, to apply to the fields such as gas absorption,[22,23,26,27] conductivity,[28] emission colors,[29−32] catalytic ability,[33] and drug delivery.[34]

The studies aimed at the antenna system with coordination bond have been leading to the multichromophoric compounds. Examples are the connection of hetero d^6 metal polypyridyl units[35] or integration of strongly phosphorescent ligands using lanthanide ions.[14−16] The linkage of luminescent molecules by coordination bonds is synthetically more feasible and causes smaller perturbation to their electronic states than that by covalent bonds, and the structural stability of coordination polymers provides the favorable pathways for energy migration. Despite such advantages to use coordination bonds to construct efficient antenna, there are still some problems to be solved. Self-quenching among concentrated chromophores,[2] which is also observed in the covalent systems, is often serious. Also, available luminescent units are still limited. Efficiency of energy transfer is not very high. Until now, the number of donor sites that can provide the collected energy to one acceptor site is around 10 at most in the coordination polymers.[14−16,35] From the viewpoint of intrinsic relief of the self-quenching, strongly luminescent coordination polymers should be certainly required as suitable candidates because their strong luminescence demonstrates that the self-quenching among luminophores is not significant.

We have been studying a series of luminescent halogeno copper(I) coordination polymers, $[Cu_2X_2(PPh_3)_2(L)]_\infty$ (X =

Received: May 30, 2015
Published: September 28, 2015

DOI: 10.1021/acs.inorgchem.5b01224
Inorg. Chem. 2015, 54, 9733−9739

Br, I), where L is N-heteroaromatic ligand.[36] They have chain structures that are characterized by diamond $\{Cu_2(\mu\text{-}X)_2\}$ cores interconnected by bridging bidentate ligands L, such as 4,4′-bipyridine (bpy). The bpy complex with X = I exhibits strong phosphorescence (quantum yield: 0.65 ± 0.1) at room temperature in the solid state. The analogous iodo silver(I) complex $[Ag_2I_2(PPh_3)_2(bpy)]_\infty$[37] also shows considerably strong phosphorescence (quantum yield: 0.72 ± 0.1) as depicted below. Another important fact is that the copper and silver μ-iodo complexes form almost identical, isomorphous crystals. This isomorphous relationship is unique and is indicative of the potentially useful candidate for the construction of the mixed-metallic coordination polymer containing two different emissive sites. The two emissive sites in one chain may act as donors and acceptors and would yield an antenna system without significant loss of emission quantum yield by structural distortion (Figure 1).

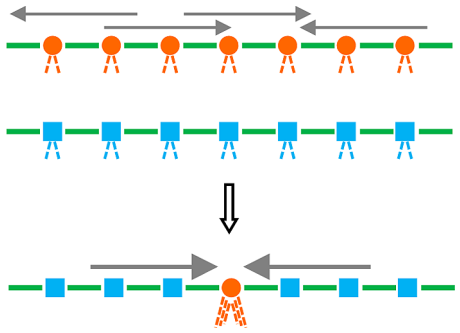

Figure 1. Formation of the luminescent mixed-metallic coordination polymer as a linear chain including donor (blue) and acceptor (orange) sites.

We could in fact prepare a series of isomorphous mixed-metallic copper(I)−silver(I) coordination polymers in various ratios of the two metal ions. They are all strongly emissive, their quantum yields even exceeding those of the parent polymers, and the efficient energy transfer from the silver(I) to the copper(I) sites is in fact observed. These unusual results are reported here.

EXPERIMENTAL SECTION

Materials. AgI (>99.87%, Cu content <0.005%) was purchased from Kojima Chemicals Co. CuI (99.5%), bpy, and organic solvents were purchased from Wako. The Cu homometallic complex was prepared as described in our previous report.[36] The Ag homometallic complex was prepared according to the literature,[37] using a CH_3CN/DMF (1:4) mixed solvent.

$[\{(Cu_xAg_{(1-x)})_2I_2(PPh_3)_2\}(bpy)]_\infty$ (x = 0.5). AgI (12.4 mg, 0.053 mmol) and PPh_3 (28.5 mg, 0.109 mmol) were dissolved in DMF (32 mL). CuI (9.8 mg, 0.051 mmol) and PPh_3 (27.3 mg, 0.104 mmol) were dissolved into CH_3CN (8 mL). To the combined solution was added bpy (47.7 mg, 0.305 mmol) in CH_3CN (1 mL). After a few days, the yellow solution afforded the yellow crystals. Yield: 46.2 mg.

Anal. Calcd for $[\{(Cu_{0.5}Ag_{0.5})_2I_2(PPh_3)_2\}(bpy)]_\infty$: C, 49.96; H, 3.46; N, 2.53. Found: C, 49.76; H, 3.50; N, 2.56. Single-crystal X-ray analysis showed the ratio of Cu:Ag = 0.497(5):0.503(5).

$[\{(Cu_xAg_{(1-x)})_2I_2(PPh_3)_2\}(bpy)]_\infty$ (x = 0.15). CuI (2.0 mg, 0.011 mmol), AgI (9.3 mg, 0.040 mmol), and PPh_3 (26.7 mg, 0.102 mmol) were dissolved in CH_3CN/DMF mixed solvent (8 mL/32 mL). To the solution was added bpy (23.9 mg, 0.153 mmol) in CH_3CN (1 mL). After a few days, the yellow solution afforded the yellow crystals. Yield: 16.3 mg.

Anal. Calcd for $[\{(Cu_{0.15}Ag_{0.85})_2I_2(PPh_3)_2\}(bpy)]_\infty$: C, 48.59; H, 3.37; N, 2.46. Found: C, 48.57; H, 3.47; N, 2.17. Single-crystal X-ray analysis showed the ratio of Cu:Ag = 0.155(4):0.845(4).

$[\{(Cu_xAg_{(1-x)})_2I_2(PPh_3)_2\}(bpy)]_\infty$ with x Smaller than 0.01. As above, to the DMF solution containing AgI (10 mg, 0.044 mmol) and PPh_3 (23 mg, 0.089 mmol) was added the CH_3CN solution of y equiv of CuI and $2y$ equiv of PPh_3. Addition of a CH_3CN solution of bpy (20 mg, 0.13 mmol) afforded the pale yellow to almost colorless crystals.

For these complexes, the elemental analysis of CHN values is substantially the same as that of the silver homometallic complex (C, 48.03; H, 3.33; N, 2.44) showing that the complexes contain mainly Ag(I) ion as metal centers. The concentration of Cu was determined by the ICP analysis after decomposition of complexes by concentrated HNO_3/H_2SO_4 aq. As shown in Table S1, the mole fraction of copper (x) in each complex is comparable to the reaction ratio in order but a slightly smaller value (1/2−1/3 of y). The mole fraction of x was determined as 0.0002, 0.0004, 0.0006, 0.0012, and 0.0052 for the complexes obtained by the reaction where y = 0.005, 0.0010, 0.0020, 0.004, and 0.01, respectively.

$[Ag_2Br_2(PPh_3)_2\}(bpy)]_\infty$. AgBr (6.3 mg, 0.033 mmol) and PPh_3 (17.5 mg, 0.066 mmol) were dissolved in a mixed solvent of CH_3CN/DMF (4 mL, 16 mL), to which was added an CH_3CN solution of bpy (1.0 mL, 18 mg, 0.12 mmol). After a few days, the solution afforded colorless crystals. Yield: 9.3 mg.

Anal. Calcd for $[Ag_2Br_2(PPh_3)_2(bpy)]_\infty$: C, 52.30; H, 3.63; N, 2.65. Found: C, 52.40; H, 3.72; N, 2.66.

The corresponding iodo complex, $[Ag_2I_2(PPh_3)_2(bpy)]_\infty$, was prepared by a similar method. Anal. Calcd for $[Ag_2I_2(PPh_3)_2(bpy)]_\infty$: C, 48.03; H, 3.33; N, 2.44. Found: C, 48.00; H, 3.39; N, 2.42.

$[Ag_2(I_{0.5}Br_{0.5})_2(PPh_3)_2\}(bpy)]_\infty$. AgI (3.9 mg, 0.017 mmol) and PPh_3 (8.8 mg, 0.033 mmol) were dissolved in a mixed solvent of CH_3CN/DMF (3.0 mL, 12 mL). AgBr (3.2 mg, 0.016 mmol) and PPh_3 (8.8 mg, 0.033 mmol) were dissolved in a mixed solution of CH_3CN/DMF (2.5 mL, 7.5 mL). To the combined solution was added bpy (18 mg, 0.12 mmol) in CH_3CN (1 mL). After a few days, the reaction solution afforded colorless crystals. Yield: 5.2 mg.

Anal. Calcd for $[Ag_2(I_{0.5}Br_{0.5})_2(PPh_3)_2\}(bpy)]_\infty$: C, 50.08; H, 3.47; N, 2.54. Found: C, 49.89; H, 3.39; N, 2.57.

Crystal Structure Analysis. Suitable single crystals of $[\{(Cu_xAg_{(1-x)})_2I_2(PPh_3)_2\}(bpy)]_\infty$ (x = 0, 0.15, 0.50, 1) were obtained as described above. The selected crystals were mounted onto thin glass fibers or loops. Measurements of the crystals with x = 0.15 and 0.50 were made on a Rigaku VariMax RAPID-DW/NAT with Cu Kα radiation at −120 °C. Although the structures of copper and silver homometallic complexes at room temperature have been reported,[36,37] the structures were determined at −120 °C for comparison. Final cell parameters were obtained from a least-squares analysis of reflections with $I > 10\sigma(I)$. Space group determinations were made on the basis of systematic absences, a statistical analysis of intensity distribution, and the successful solution and refinement of the structures. Data were collected and processed using CrystalClear and RapidAuto. An empirical absorption correction resulted in acceptable transmission factors. The data were corrected for Lorentz and polarization factors.

All of the calculations were carried out using CrystalStructure[39] and SHELX-97.[40] The ORTEP diagrams of the structures were prepared by using ORTEP-III.[41] The structures were solved by direct methods and expanded using Fourier and difference Fourier techniques. In the mixed-metallic compounds, copper and silver atoms were set at the same position with the same displacement factors, and the ratios of occupation factors were refined. Details of crystal parameters and structure refinement are given in Table S2. Selected bond lengths and angles are shown in Table 1.

CCDC-990694, 990697, 1422133, and 1422138 contain the supplementary crystallographic data for this Article. These data can be obtained free of charge via www.ccdc.cam.ac.uk/conts/retrieving/html (or from the Cambridge Crystallographic Data Centre, 12 Union Road, Cambridge CB2 1EZ, UK; fax, (+44)1223-336-033; or e-mail, deposit@ccdc.cam.ac.uk).

DOI: 10.1021/acs.inorgchem.5b01224
Inorg. Chem. 2015, 54, 9733−9739

Table 1. Bond Distances (Å) around the Metal Center in Homo- and Mixed-Metallic Complexes $[\{(Cu_xAg_{(1-x)})_2I_2(PPh_3)_2\}(bpy)]$ Measured at −120 °C

	x			
	0	0.15	0.5	1
M−I	2.8198(5)	2.7879(7)	2.7204(8)	2.6552(11)
	2.9191(5)	2.8944(7)	2.8410(8)	2.7330(11)
M−P	2.4435(11)	2.4161(15)	2.3527(16)	2.2376(16)
M−N	2.368(4)	2.324(5)	2.254(6)	2.078(6)
M···M	3.1040(7)	3.0969(6)	3.0809(8)	3.1012(15)

Photophysical Measurements. Emission spectra were measured by using a photodiode array detector (Hamamatsu, PMA-11) and an Nd:YAG laser (Continuum surelite, 355 nm, 7 ns pulse width) at 355 nm excitation. Emission lifetimes were measured by using a streak camera (Hamamatsu C3434) as a detector. Photoluminescent quantum yields were measured at room temperature in the solid state with the integrating sphere at 355 nm excitation (Hamamatsu, C9920-03).

RESULTS AND DISCUSSION

Synthesis and Structures. The copper and silver homometallic complexes, $[Cu_2I_2(PPh_3)_2(bpy)]_\infty$ and $[Ag_2I_2(PPh_3)_2(bpy)]_\infty$, have been synthesized as yellow and colorless single crystals, respectively, by the reaction of the corresponding metal(I) iodide, PPh_3, and bpy in DMSO at room temperature.[37,38] By the same method with varying ratio of copper iodide and silver iodide in solution, a series of iodo copper(I)−silver(I) mixed-metallic coordination polymers with various mole fraction of copper(I) (x) ranging from 0.5 to 0.0002 was prepared. The mixed-metallic complexes were obtained as single crystals substantially colorless to yellow depending on the mole fraction of copper(I).

As revealed by their lattice constants, the parent copper and silver complexes form isomorphous crystals (Table S2). The difference is less than 3.5% for each lattice constant, and the difference of cell volume is 3.3% (Table S2). Although the M−I, M−P, and M−N distances (M = Cu, Ag) are longer in the silver complex by about 0.2−0.3 Å, reflecting the difference of the ionic radii, the total arrangement of ligands and the polymeric chain are practically the same in the two homometallic crystals (Table 1 and Figure 2).

In addition to the isomorphous relationship, the similar solubilities of parent compounds and the lability of copper(I) and silver(I) ions assist the straightforward synthesis of mixed Ag−Cu complexes. As expected from the isomorphous relationship between the parent complexes, a series of mixed-metallic complexes was obtained as isomorphous crystals with the homometallic ones (Table S2). The copper(I) and silver(I) ions occupy the same crystallographic site in the mixed-metallic complexes, implying the formation of polymeric chains containing both copper and the silver sites (Figure 2). In the case of the 1:1 mixed-metallic complex, the bond distances around metal ions are the average values of the parent complexes (Table 1), which also indicates the statistical distribution of copper(I) and silver(I) ions in the chain.

Luminescent Properties of Mixed-Metallic Complexes. Figure 3 shows the emission spectra of the mixed-metallic compounds at room temperature upon excitation at 355 nm, together with those of the parent homometallic complexes.

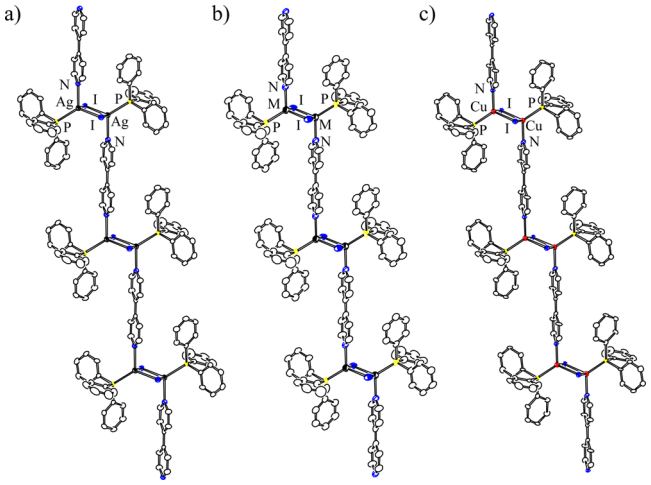

Figure 2. ORTEP[41] diagrams of homo- and mixed-metallic complexes in 50% probability: (a) Ag complex, (b) mixed-metallic complex (x = 0.5), and (c) Cu complex. The hydrogen atoms are omitted for clarity.

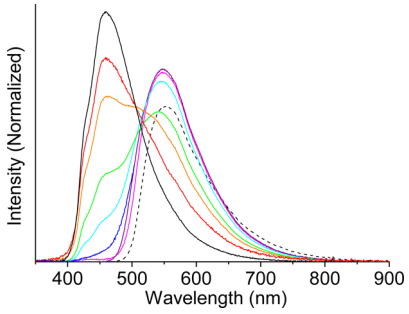

Figure 3. Emission spectra of mixed-metallic compounds and the homometallic compounds at room temperature (λ_{ex} = 355 nm); red, x = 0.0002; orange, x = 0.0004; green, x = 0.0006; sky blue, x = 0.0012; blue, x = 0.0052; pink, x = 0.15; purple, x = 0.5; black (solid), silver compound; black (broken), copper compound. Emission intensities are normalized with respect to the luminescence quantum yields.

The parent silver complex shows a strong emission peak at 450 nm assignable to the $\pi-\pi^*$ transition with the quantum yield of 0.72 ± 0.1 and lifetime of 18.7 μs. The copper complex shows strong MLCT emission at 530 nm with the quantum yield and lifetime of 0.65 ± 0.1 and 4.0 μs, respectively. Their emission lifetimes indicate the triplet nature of their excited states.[36,42] All of the mixed-metallic complexes retain strong emissions with the peaks at the wavelength corresponding to either or both of the original homometallic polymers (vide infra). The 1:1 mixed-metallic complex (x = 0.5) shows an emission band identical to that of the homometallic copper(I) complex. Even the complex with x = 0.15 (Ag of 85%) gives an emission spectrum identical to that of the homometallic copper(I) complex. Along with the further decrease of x, the characteristic bands corresponding to copper(I) and silver(I) components decreased and increased, respectively. It is surprising that a slight feature of the emission characteristic of the copper site remains below the 500 nm region as a weak shoulder until the copper content reaches as low as 0.0004. Even when x = 0.0002, all of the metal sites are substantially occupied by silver(I) ions, the band broadening due to the copper(I) component was observed, showing the remarkable sensitivity of this system to the copper component.[43] Because the emission from the silver site is substantially quenched in the

DOI: 10.1021/acs.inorgchem.5b01224
Inorg. Chem. 2015, 54, 9733−9739

complex with x = 0.0052, at least 0.5% of Cu is sufficient to quench all of the energies absorbed by the Ag sites in the mixed-metallic complex. The results imply that emission of at least ca. 200 silver units is converted into the emission of one copper unit. In other words, the copper site acts as an at least 200 times more efficient emitter in the mixed metallic complex exploiting the surrounding Ag units as donors. This quenching efficiency is quite high as compared to other light-harvesting system constructed by integration of strongly luminescent molecules,[10,16,18] and is comparable to or even slightly better than that observed for the mesoporous silica with coumarin, which is one of the best artificial light-harvesting systems so far.[9]

The coincidence of emission energies of the silver and copper sites in the mixed-metallic complexes with those of homometallic complexes indicates that the mixed-metallic complex is an independent or a weak-coupled system containing two different emissive excited states in one chain. Such a "localized" character of the excited states in the present polymeric complexes is also supported by the similarity of luminescent properties between the Cu homometallic polymers and the corresponding molecular complexes, $[Cu_2(\mu\text{-}X)_2(PPh_3)_2(L)_2$ (X = I, Br, Cl; L = monodentate N-heteroaromatic ligands).[36,42] As revealed by the crystal structure determination, the metal sites in the mixed-metallic complexes are occupied by Cu(I) or Ag(I) ions statistically. It is reasonable to assume statistical formation of the mixed-metallic $\{CuAg(\mu\text{-}I)_2\}$ units in addition to the homometallic $\{M_2(\mu\text{-}I)_2\}$ (M = Cu, Ag) ones, rather than the statistical distribution of the two homometallic dimeric units. The observation of the MLCT emission band in the same energy for the mixed-metallic compounds indicates that the Cu−Ag or the Cu−Cu and Ag−Ag interactions in the units are not significant, probably because of the large metal metal separation (d_{Cu-Cu}, 3.1040(7) Å; d_{Ag-Ag}, 3.1012(15) Å) in the $\{M_2(\mu\text{-}I)_2\}$ core, although Cu−Cu interaction has been reported to play an important role in emissive properties of multinuclear copper(I) complexes.[44]

In addition to the high sensitivity of the emission peaks to the mole fraction of copper(I) ion, preservation of highly efficient photoluminescence is another feature of this system. As shown in Table 2, the homometallic complexes show relatively high quantum yields of 0.72 ± 0.1 and 0.65 ± 0.1 for the silver and the copper complexes, respectively, whereas the mixed-metallic complexes show the apparent quantum yields around 0.8 ± 0.1. The isomorphous relationship, which does not provoke the structural distortion that usually leads to the decrease in the quantum yield, should play an important role in the preservation of high luminescent quantum yield in the present case. The enhancement of quantum yields in the mixed-metallic complexes with x = 0.5 and 0.15 is worth noting because they show a spectrum identical to that of the copper(I) homometallic complex. It may imply the larger intrinsic emissive ability of the copper(I) site, which is less self-quenched in the mixed-metallic complexes than in the homometallic copper complex.

Table 2. Luminescent Quantum Yield (Φ) of Mixed-Metallic and Homometallic Complexes

molar ratio of Cu (x)	Ag (%)	Φ
1	0	0.65 ± 0.1
0.5	50	0.74 ± 0.1
0.15	85	0.77 ± 0.1
0.0052	99.5	0.75 ± 0.1
0.0012	99.9	0.80 ± 0.1
0.0006	>99.9	0.75 ± 0.1
0.0004	>99.9	0.84 ± 0.1
0.0002	>99.9	0.80 ± 0.1
0	100	0.72 ± 0.1

Energy Migration among Emissive Units. To discuss the energy migration process in detail, the flash photolysis was performed. Figure 4 shows the time-gated spectra of mixed-metallic complex with x = 0.0006. In the early gated spectrum (0−5 μs), the larger contribution from the band of the silver site was observed as expected from its stationary luminescence spectrum (Figure 3, green line). On the other hand, the emission in the late-gated spectrum (30−50 μs) was mainly composed of the band characteristic of the copper site. Other mixed-metallic complexes having both bands corresponding to the copper and the silver sites (x = 0.0002, 0.0004, 0.0012) showed similar time-gated spectra (Figures S3 and S4).

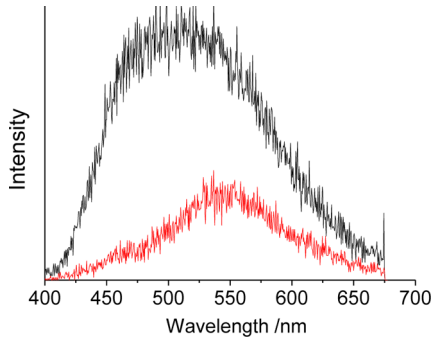

Figure 4. Time-gated spectra of mixed-metallic complex with x = 0.0006; black, early gated (0−5 μs); red, late gated (30−50 μs).

Because the homometallic silver complex has a longer lifetime (18.7 μs) than the homometallic copper complex (4.0 μs), the dominant emission in the late-gated spectrum should be that of the silver site if each site emits without any communication. The appearance of emission characteristic of the copper site in the late-gated spectrum manifests that the energy transfer from the silver sites to the copper sites occurs in the mixed-metallic complexes.

Figure 5 shows the emission decays of the 400−480 and the 550−650 nm regions of the mixed-metallic complex with x = 0.0006, with the former and the latter regions corresponding to

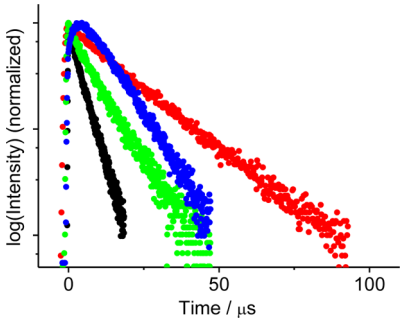

Figure 5. Emission decay curves of the mixed-metallic complex (x = 0.0006) and the homometallic compounds. Black, copper compound; red, silver compound; green, mixed-metallic compound (400−480 nm); blue, mixed-metallic compound (550−650 nm).

DOI: 10.1021/acs.inorgchem.5b01224
Inorg. Chem. 2015, 54, 9733−9739

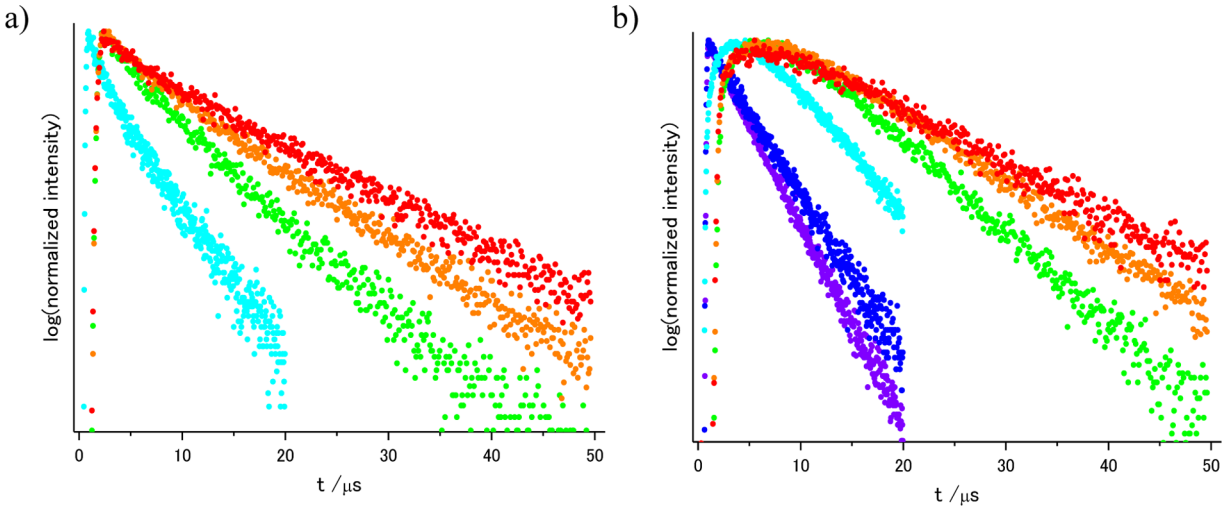

Figure 6. Emission decays of mixed-metallic complexes $[\{(Cu_xAg_{(1-x)})_2I_2(PPh_3)_2\}(bpy)]_\infty$: (a) 400−480 nm, (b) 550−650 nm; violet, x = 0.5; blue, x = 0.15; sky blue, x = 0.0012; green, x = 0.0006; orange, x = 0.0004; red, x = 0.0002.

the emission from the silver and the copper sites, respectively. While the decay curve of the former region monotonously decreased, that of the latter region showed the "rise", increased until 5 μs. The increase corresponds to the increase of the excited state of the copper site in the absence of excitation light, demonstrating the energy migration from the silver to the copper sites.

The emission decays of both regions were satisfactorily reproduced with double-exponential functions to afford apparent rate constants of 1.1×10^5 s^{-1} (τ = 9.1 μs) and 4.6×10^5 s^{-1} (τ = 2.2 μs) for the former energy region, and 1.0×10^5 s^{-1} (τ = 9.6 μs) and 3.4×10^5 s^{-1} (τ = 3.0 μs) for the latter. For other mixed-metallic compounds with x = 0.0002−0.0012, which showed the characteristic emission bands of both the silver and the copper components, the rise in the emission decay curves corresponding to the copper sites was also observed (Figure 6).

The emission decay curves of the two regions were also fitted with double-exponential functions for these complexes. The slower component of both regions gradually approached that of the silver(I) homometallic complex along with the decrease of x. On the other hand, for the mixed-metallic complexes that show practically only a copper emission band (x = 0.15 and 0.5), the emission decay curve was monotonously decreased to be fitted with a single exponential function. The apparent emission lifetime is, however, longer than that of the copper(I) homometallic complex. It is worth noting that for the complexes that show double exponential decays, two slower decay rate constants of the higher and lower energy regions are in good agreement with each other, and similarly for two faster rate constants (Table 3). This behavior is reminiscent of the emission decays explained by the traditional Birks two-state scheme where the apparent emission lifetimes are derived from energy migration rate between two states and the decay constant of each state.[45,46]

Because neighboring chains are separated by bulky triphenylphosphine ligands and because the related excited states are triplet, we conclude that the intrachain migration by Dexter mechanism is dominant in the present system. The contribution of Forster type energy migration as implied by the overlap of the emission band of the silver complex (Figure 3) and the absorption band of the copper complex (Figure S5) would not be important as a very minor singlet character should be involved in the excited states.

Table 3. Apparent Emission Decay Constants for Mixed-Metallic Complexes

	silver region (400−480 nm)		copper region (550−650 nm)	
mole fraction of Cu, x	τ_1/μs	τ_2/μs	τ_1/μs	τ_2/μs
1.0			4.0	
0.5			4.3	
0.15			5.3	
0.0052	3.7	0.68	5.6	0.74
0.0012	5.9	1.0	7.3	2.0
0.0006	9.1	2.2	9.6	3.0
0.0004	13	3.3	13	3.4
0.0002	17	3.3	16	3.1
0	18			

The intrachain energy migration processes can be separated into the energy transfer between the same neighboring sites $k_{Cu\to Cu}$ and $k_{Ag\to Ag}$, and between different neighboring sites $k_{Ag\to Cu}$ and $k_{Cu\to Ag}$. Here, the energy migration among the same site is assumed to be fast enough not to be the rate-determining step.[47] The energy transfer processes in the chain then depend on the lifetime of each excited state, the energy transfer rates between different neighboring sites, and the concentration of copper sites. The energy transfer rate constants were evaluated by applying similar type equations to the Birks mechanism. In the present system, the effective energy transfer rates between the two excited states are represented to be proportional to the ratio of metal ions (Supporting Information, Appendix). The analysis showed that the apparent rate constants were well reproduced when the energy transfer rates were assumed as $k_{Ag\to Cu} = 1.1(2) \times 10^8$ s^{-1} and $k_{Cu\to Ag} = 1.0(3) \times 10^5$ s^{-1} (Figure 7).

Therefore, the energy migration rate from the silver site to the copper site ($k_{Ag\to Cu}$) is about 10^3 times larger than the reverse one ($k_{Cu\to Ag}$), which explains the efficient energy transfer from the silver site to the copper site and the remarkable sensitivity to the copper concentration of this system. Because the energy migration rate is dependent on the overlap of the emission band of the donor site and the

DOI: 10.1021/acs.inorgchem.5b01224
Inorg. Chem. 2015, 54, 9733−9739

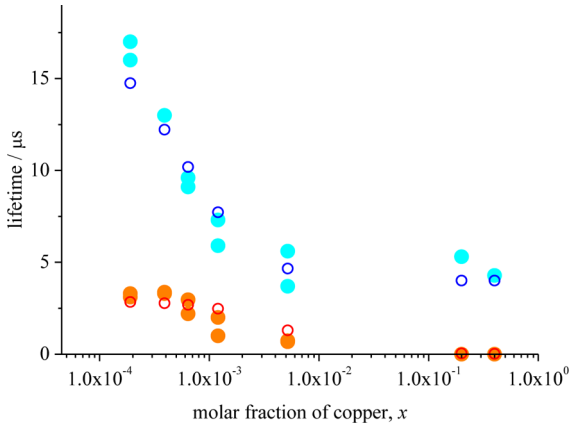

Figure 7. Plot of the apparent lifetime versus mole fraction of copper. The calculated values are overlaid. Evaluation details are described in the Supporting Information. Sky blue ●, τ_1(obsd); orange ●, τ_2(obsd); blue ○, τ_1(calcd); red ○, τ_2(calcd).

absorption band of the acceptor site in Dexter mechanism, the slower energy migration rate from the copper site to the silver site would be the result of a substantial lack of the overlap between the emission band of the copper site and the absorption band of the silver site (Figures 3 and S5). Because the energy transfer rate from the antenna (silver site) to the acceptor (copper site) is not very fast in the present system, the highly efficient energy concentration to the copper site is due to the rather small rate constant of the back reaction, while the phosphorescent units have a longer lived excited state.

CONCLUSION

In this Article, we report a series of copper(I)−silver(I) mixed-metallic coordination polymers by exploring the isomorphous relationship between the strongly luminescent homometallic copper(I) and silver(I) compounds. The mixed-metallic complexes also show high luminescent quantum yields, and their luminescent properties are significantly sensitive to the amount of copper component, with emission characteristics of the copper sites being observed in the samples with the copper content even as low as 0.005. The examination of luminescent spectra and lifetimes together with the time-resolved spectra confirm the efficient energy transfer from the silver sites to the copper sites showing that the system can be regarded as an efficient light-harvesting system with silver sites as the antenna and copper sites as the acceptors. As mentioned in the Introduction, ligand- and metal-mixed luminescent coordination polymers have been utilized for various applications.[21−23,25−33] The present study adds an excellent example of coordination polymers in the field of the photoantenna system. Because the photoactive metal-complex units do not necessarily require the strongly luminescent ligands or metal centers, the integration of metal complex units to the light-harvesting system will allow for the utilization of a wider range of molecules and metals as the active components.

ASSOCIATED CONTENT

Supporting Information

The Supporting Information is available free of charge on the ACS Publications website at DOI: 10.1021/acs.inorgchem.5b01224.

Experimental details, tables of crystallographic data, figures of emission spectra, time-gated spectra, and emission decays (PDF)
X-ray data for $C_{46}H_{38}Ag_2I_2N_2P_2$ (CIF)
X-ray data for $C_{46}H_{38}Ag_{1.7}Cu_{0.3}I_2N_2P_2$ (CIF)
X-ray data for $C_{46}H_{38}AgCuI_2N_2P_2$ (CIF)
X-ray data for $C_{46}H_{38}Cu_2I_2N_2P_2$ (CIF)

AUTHOR INFORMATION

Corresponding Authors

*E-mail: tsuge@sci.u-toyama.ac.jp.
*E-mail: ysasaki@sci.hokudai.ac.jp.

Notes

The authors declare no competing financial interest.

ACKNOWLEDGMENTS

This work was partly supported by a Grant-in-Aid for Scientific Research on Innovative Areas (no. 15H00868 to K.T.) as well as a Grant-in-Aid for Scientific Research (C) (no. 15K05448 to K.T.). Ayako Watanabe is acknowledged for her help in IPC measurements.

REFERENCES

(1) Frischmann, P. D.; Mahata, K.; Würthner, F. *Chem. Soc. Rev.* **2013**, *42*, 1847−1870.
(2) Rao, K. V.; Datta, K. K. R.; Eswaramoorthy, M.; George, S. J. *Chem. - Eur. J.* **2012**, *18*, 2184−2194.
(3) Wong, W.-Y.; Ho, C.-L. *Acc. Chem. Res.* **2010**, *43*, 1246−1256.
(4) Thompson, B. C.; Fréchet, J. M. J. *Angew. Chem., Int. Ed.* **2008**, *47*, 58−77.
(5) Sun, Y.; Giebink, N. C.; Kanno, H.; Ma, B.; Thompson, M. E.; Forrest, S. R. *Nature* **2006**, *440*, 908−912.
(6) McDermott, G.; Prince, S. M.; Freer, A. A.; Hawthornthwaite-Lawless, A. M.; Papiz, M. Z.; Cogdell, R. J.; Isaacs, N. W. *Nature* **1995**, *374*, 517−521.
(7) Calzaferri, G.; Huber, S.; Maas, H.; Minkowski, C. *Angew. Chem., Int. Ed.* **2003**, *42*, 3732−3758.
(8) Mizoshita, N.; Tani, T.; Inagaki, S. *Chem. Soc. Rev.* **2011**, *40*, 789−800.
(9) Inagaki, S.; Ohtani, O.; Goto, Y.; Okamoto, K.; Ikai, M.; Yamanaka, K.; Tani, T.; Okada, T. *Angew. Chem., Int. Ed.* **2009**, *48*, 4042−4046.
(10) Zeng, Y.; Li, Y.-Y.; Chen, J.; Yang, G.; Li, Y. *Chem. - Asian J.* **2010**, *5*, 992−1005.
(11) Choi, M.-S.; Yamazaki, T.; Yamazaki, I.; Aida, T. *Angew. Chem., Int. Ed.* **2004**, *43*, 150−158.
(12) Hoeben, F. J. M.; Jonkheijm, P.; Meijer, E. W.; Schenning, A. P. H. *Chem. Rev.* **2005**, *105*, 1491−1546.
(13) Huynh, M. H. V.; Dattelbaum, D. M.; Meyer, T. J. *Coord. Chem. Rev.* **2005**, *249*, 457−483.
(14) Zhang, X.; Chen, Z.-K.; Loh, K. P. *J. Am. Chem. Soc.* **2009**, *131*, 7210−7211.
(15) Zhang, X.; Ballem, M. A.; Ahrén, M.; Suska, A.; Bergman, P.; Uvdal, K. *J. Am. Chem. Soc.* **2010**, *132*, 10391−10397.
(16) Zhang, X.; Ballem, M. A.; Hu, Z.-J.; Bergman, P.; Uvdal, K. *Angew. Chem., Int. Ed.* **2011**, *50*, 5729−5733.
(17) Chrisstoffels, L. A. J.; Adronov, A.; Fréchet, J. M. J. *Angew. Chem., Int. Ed.* **2000**, *39*, 2163−2167.
(18) Ishida, Y.; Shimada, T.; Masui, D.; Tachibana, H.; Inoue, H.; Takagi, S. *J. Am. Chem. Soc.* **2011**, *133*, 14280−14286.
(19) Ajayaghosh, A.; Praveen, V. K.; Vijayakumar, C. *Chem. Soc. Rev.* **2008**, *37*, 109−122.
(20) (a) Tranchemontagne, D. J.; Mendoza-Cortés, J. L.; O'Keeffe, M.; Yaghi, O. M. *Chem. Soc. Rev.* **2009**, *38*, 1257−1283. (b) Horike, S.; Shimomura, S.; Kitagawa, S. *Nat. Chem.* **2009**, *1*, 695−704.
(21) Burrows, A. D. *CrystEngComm* **2011**, *13*, 3623−3642.

DOI: 10.1021/acs.inorgchem.5b01224
Inorg. Chem. 2015, 54, 9733−9739

(22) Deng, H.; Doonan, C. J.; Furukawa, H.; Ferreira, R. B.; Towne, J.; Knobler, C. B.; Wang, B.; Yaghi, O. M. *Science* **2010**, *327*, 846−850.
(23) Foo, M. L.; Matsuda, R.; Kitagawa, S. *Chem. Mater.* **2014**, *26*, 310−322.
(24) (a) *Intermetallic Compounds: Principles and Practice*; Westbrook, J. H., Fleischer, R. L., Eds.; Wiley: New York, 1995; Vol. *1*. (b) Schröter, W. *Electronic Structure and Properties of Semiconductors*; VCH: New York, 1991. (c) *Phosphor Handbook*, 2nd ed.; Yen, W. M., Shionoya, S., Yamamoto, H., Eds.; CRC Press: New York, 2007.
(25) (a) Burrows, A. D.; Fisher, L. C.; Richardson, C.; Rigby, S. P. *Chem. Commun.* **2011**, *47*, 3380−3382. (b) Kleist, W.; Jutz, F.; Maciejewski, M.; Baiker, A. *Eur. J. Inorg. Chem.* **2009**, *2009*, 3552−3561. (c) Vujovic, D.; Raubenheimer, H. G.; Nassimbeni, L. R. *Eur. J. Inorg. Chem.* **2004**, *2004*, 2943−2949. (d) Zeng, M.-H.; Wang, B.; Wang, X.-Y.; Zhang, W.-X.; Chen, X.-M.; Gao, S. *Inorg. Chem.* **2006**, *45*, 7069−7076.
(26) Fukushima, T.; Horike, S.; Inubushi, Y.; Nakagawa, K.; Kubota, Y.; Takata, M.; Kitagawa, S. *Angew. Chem., Int. Ed.* **2010**, *49*, 4820−4824.
(27) (a) Wang, C.; Xie, Z.; deKrafft, K. E.; Lin, W. *J. Am. Chem. Soc.* **2011**, *133*, 13445−13454. (b) Botas, J. A.; Calleja, G.; Sanchez-Sanchez, M.; Orcajo, M. G. *Langmuir* **2010**, *26*, 5300−5303. (c) Li, H. H.; Shi, W.; Zhao, K. N.; Li, H.; Bing, Y. M.; Cheng, P. *Inorg. Chem.* **2012**, *51*, 9200−9207. (d) Chun, H.; Dybtsev, D. N.; Kim, H.; Kim, K. *Chem. - Eur. J.* **2005**, *11*, 3521−3529. (e) Wu, T.; Bu, X.; Zhang, J.; Feng, P. *Chem. Mater.* **2008**, *20*, 7377−7382.
(28) Matsuzaki, H.; Iwano, K.; Aizawa, T.; Ono, M.; Kishida, H.; Yamashita, M.; Okamoto, H. *Phys. Rev. B: Condens. Matter Mater. Phys.* **2004**, *70*, 035204.
(29) (a) Falcaro, P.; Furukawa, S. *Angew. Chem., Int. Ed.* **2012**, *51*, 8431−8433. (b) Rao, X. T.; Huang, Q.; Yang, X. L.; Cui, Y. J.; Yang, Y.; Wu, C. D.; Chen, B. L.; Qian, G. D. *J. Mater. Chem.* **2012**, *22*, 3210−3214. (c) Sendor, D.; Hilder, M.; Juestel, T.; Junk, P. C.; Kynast, U. H. *New J. Chem.* **2003**, *27*, 1070−1077. (d) de Lill, D. T.; de Bettencourt-Dias, A.; Cahill, C. L. *Inorg. Chem.* **2007**, *46*, 3960−3965. (e) Soares-Santos, P. C. R.; Cunha-Silva, L.; Almeida Paz, F. A.; Sá Ferreira, R. A.; Rocha, J.; Trindade, T.; Carlos, L. D.; Nogueira, H. I. S. *Cryst. Growth Des.* **2008**, *8*, 2505−2516. (f) Thirumurugan, A.; Cheetham, A. K. *Eur. J. Inorg. Chem.* **2010**, *2010*, 3823−3828. (g) Liu, K.; You, H.; Zheng, Y.; Jia, G.; Song, Y.; Huang, Y.; Yang, M.; Jia, J.; Guo, N.; Zhang, H. *J. Mater. Chem.* **2010**, *20*, 3272−3279. (h) Hirai, Y.; Nakanishi, T.; Miyata, K.; Fushimi, K.; Hasegawa, Y. *Mater. Lett.* **2014**, *130*, 91−93.
(30) Kerbellec, N.; Kustaryono, D.; Haquin, V.; Etienne, M.; Daiguebonne, C.; Guillou, O. *Inorg. Chem.* **2009**, *48*, 2837−2843.
(31) Rybak, J.-C.; Hailmann, M.; Matthes, P. R.; Zurawski, A.; Nitsch, J.; Steffen, A.; Heck, J. G.; Feldmann, C.; Götzendörfer, S.; Meinhardt, J.; Sextl, G.; Kohlmann, H.; Sedlmaier, S. J.; Schnick, W.; Müller-Buschbaum, K. *J. Am. Chem. Soc.* **2013**, *135*, 6896−6902.
(32) (a) Colis, J. C. F.; Larochelle, C.; Fernandez, E. J.; Lopez-de-Luzuriaga, J. M.; Monge, M.; Laguna, A.; Tripp, C.; Patterson, H. *J. Phys. Chem. B* **2005**, *109*, 4317−4323. (b) Hettiarachchi, S. R.; Schaefer, B. K.; Yson, R. L.; Staples, R. J.; Herbst-Irmer, R.; Patterson, H. H. *Inorg. Chem.* **2007**, *46*, 6997−7004. (c) Lu, H.; Yson, R.; Ford, J.; Tracy, H. J.; Carrier, A. B.; Keller, A.; Mullin, J. L.; Poissan, M. J.; Sawan, S.; Patterson, H. H. *Chem. Phys. Lett.* **2007**, *443*, 55−60. (d) Colis, J. C. F.; Larochelle, C.; Staples, R.; Herbst-Irmer, R.; Patterson, H. H. *Dalton Trans.* **2005**, 675−679.
(33) Marx, S.; Kleist, W.; Huang, J.; Maciejewski, M.; Baiker, A. *Dalton Trans.* **2010**, *39*, 3795−3798.
(34) Taylor-Pashow, K. M. L.; Rocca, J. D.; Xie, Z.; Tran, S.; Lin, W. *J. Am. Chem. Soc.* **2009**, *131*, 14261−14263.
(35) (a) Kent, C. A.; Mehl, B. P.; Ma, L.; Papanikolas, J. M.; Meyer, T. J.; Lin, W. *J. Am. Chem. Soc.* **2010**, *132*, 12767−12769. (b) Barrett, S. M.; Wang, C.; Lin, W. *J. Mater. Chem.* **2012**, *22*, 10329−10334.
(36) Araki, H.; Tsuge, K.; Sasaki, Y.; Ishizaka, S.; Kitamura, N. *Inorg. Chem.* **2005**, *44*, 9667−9675.
(37) Sampanthar, J. T.; Vittal, J. J. *Cryst. Eng.* **2000**, *3*, 117−133.
(38) Li, R.-Z.; Li, D.; Huang, X.-C.; Qi, Z.-Y.; Chen, X.-M. *Inorg. Chem. Commun.* **2003**, *6*, 1017−1019.
(39) Crystal Structure Analysis Package, Rigaku Corp. (2000−2010), Tokyo 196-8666, Japan.
(40) Sheldrick, G. M. A. *Acta Crystallogr., Sect. A: Found. Crystallogr.* **2008**, *64*, 112−122.
(41) Burnett. M. N.; Johnson, C. K. Oak Ridge National Laboratory Report ORNL-6895, 1996.
(42) (a) Tsuge, K.; Chishina, Y.; Hashiguchi, H.; Sasaki, Y.; Kato, M.; Ishizaka, S.; Kitamura, N. *Coord. Chem. Rev.*, in print (doi: 10.1016/j.ccr.2015.03022). (b) Tsuge, K. *Chem. Lett.* **2013**, *42*, 204−208.
(43) Because of the very low content of Cu to Ag, it is not clear if Cu is really included in the crystals or involved as impurity; we have carried out further experiment to confirm that the photophysical measurements reported herein are intrinsic. These experimental results are reported in the Supporting Information.
(44) Ford, P. C.; Cariati, E.; Bourassa, J. *Chem. Rev.* **1999**, *99*, 3625−3648.
(45) Birks, J. B. *Photophysics of Aromatic Molecules*; Wiley: New York, 1970; p 301.
(46) Winnik, M. A. *Acc. Chem. Res.* **1985**, *18*, 73−79.
(47) This assumption is well supported by the fact that the mixed-halogeno iodo−bromo silver(I) complex shows the single exponential decay with the averaged lifetimes of the parent complexes (Figure S6).

DOI: 10.1021/acs.inorgchem.5b01224
Inorg. Chem. 2015, 54, 9733−9739